Acta Technica 62 (2017), No. 7A, 1139–1150

Joint trajectory tracking prediction based on complex number weight network

Lizheng Liu[1,2], Fangai Liu[1]

Abstract. In this paper, based on the field bicycle environment, this paper proposes a tracking algorithm for the field bicycle based on RSSI distance measurement. In order to improve the accuracy of ranging, the propagation model of log-normal distribution is adopted, and indoor / outdoor environment data are measured on the spot to estimate the environmental parameters. Then, based on the estimated environmental parameters, the propagation model is reconstructed and the distance is measured. The TCTR algorithm measures the distance between the bicycle and the coach based on the RSSI value received by the Log-normal shadowing model (LNSM) and the anchor node. In order to improve the accuracy of ranging, indoor and outdoor field cycling experiments were established to obtain RSSI value and distance data. Finally, the LNSM parameters were estimated through fitting. The simulation results show that by optimizing the LNSM parameters, the root mean square error of ranging is reduced.

Key words. Received signal strength, Normal fading model, Point of interest, fitting, Distance measurement.

1. Introduction

Location information is the key to many types of Wireless Sensor Networks (WSNs) applications such as target tracking, personal tracking, monitoring [1], health care, and environmental management [2]. At present, the commonly used WSN positioning methods are: based on ranging and non-ranging. The former can be used to estimate the distance or angle between sensing nodes, which has high accuracy, such as Angle of arrival (AoA), Time of Arrival (ToA), Time Difference of Arrival (TDoA)[3]and Received Signal Strength Indicator (RSSI).

The AoA ranging method relies on the accuracy of the omnidirectional antenna and requires the addition of additional antennas, which means an increase in cost.

[1]Shandong Normal University, Jinan 250014, Shandong, China
[2]Shandong University of Finance and Economics, Jinan 250014, Shandong, China

ToA and TDoA methods, on the other hand, require that all receiving nodes that can sense the target signal be synchronized in unison. Although TDoA has high ranging accuracy, it also requires additional hardware and consumes more energy [4]. The RSSI ranging method is simple and easy to implement, without additional equipment, does not require clock synchronization, but the ranging accuracy is low. Therefore, the accuracy of ranging can be improved by optimizing the environmental parameters that affect the accuracy of RSSI ranging. In WSNs, mobile sensing nodes are limited to energy supplies and hardware devices.Therefore, in field bicycle applications, tracking based on ranging methods is considered, and these ranging methods can be combined with ZigBee, Bluetooth, Wi-Fi and RFID devices. Compared to ZigBee, RFID is mainly used in short-range scenarios, Bluetooth has only a small coverage area, and Wi-Fi consumes more power and is not suitable for long-distance tracking. Therefore, only ZigBee can maintain ranging services with low power, low complexity, low cost and high spreading [5]. In addition, RSSI values are affected by wireless channel characteristics such as multipath, NLOS environment, fading, and interference, ultimately affecting the accuracy of the ranging. In the RSSI ranging method, if the distant transmitter moves toward the receiver, the signal strength received by the receiver will be enhanced, and vice versa. This results in a measurement error of the RSSI. The accuracy based on RSSI ranging is closely related to RSSI value of signal strength and environmental parameters. First of all, the signal strength RSSI value measured by the channel transient environment, should be measured many times, but not based on a single RSSI value, the estimated distance. Secondly, the environmental parameters are easily affected by the external environment, which is volatile. Therefore, the environmental parameters need to be estimated based on the current field environment rather than the empirical model to estimate the environmental parameters.

2. Wireless channel model and LNSM

2.1. *Wireless channel model*

RSSI value is easy to be influenced by the channel environmental. Therefore, the wireless channel model must be carefully chosen to obtain accurate RSSI values. Now there are three main channel models: free space model, dual path model and logarithm normal shadow fading model LNSM (Log-Normal Shadowing Model). The LNSM takes into account the effect of obstruction blocking on the transmitted signal and is suitable for the actual environment of the site bike. In addition, the Doppler effect must be taken into account as the tracking target is always moving. Next, analyze the effect of Doppler shift on ranging in ZigBee positioning network.

In the TCTR algorithm, the source node is fixed and the tracking target (bicycle) moves all the way. Therefore, the Doppler shift f_d depends mainly on the bicycle speed ϑ_b. Based on this situation, Doppler shift f_d can be defined [6]:

$$f_d = (\vartheta_b f_c/c)\, cos\alpha\,. \tag{1}$$

Where c is the speed of light, α is the angle between the velocity vectors of two nodes, and $\alpha \in [0, \pi]$.

To calculate the maximum Doppler shift f_d, the angle α must be zero. Based on the ZigBee protocol with 2.4 GHz ISM bandwidth, Equation (1) can be converted to:

$$\begin{aligned} f_d &= (\vartheta_b f_c/c)\cos\alpha = \left(2.4\times 10^9/3.6\left(3\times 10^8\right)\right)\vartheta_b \\ &= 2.222\vartheta_b \end{aligned} \tag{2}$$

Among them, 3.6 is from the unit of speed conversion.

In the bike area, the maximum bike speed is 60 km/h. According to equation (2), the corresponding relationship between vehicle speed and Doppler shift f_d can be obtained, as shown in Table 1.

Table 1. the relationship between speed and Doppler frequency shift f_d

Bicycle speed (km/h)	Doppler frequency shift (Hz)
5	11.1
10	22.2
15	33.3
20	44.4
25	55.5
30	66.6
35	77.7
40	88.8
45	99.9
50	111.1
55	122.2
60	133.3

As can be seen from Table 1, when the vehicle speed is 60 km/h, the Doppler frequency shift f_d is maximum to 133.3Hz, and. The ZigBee bandwidth is 2MHz [7], even the largest Doppler shift f_d is negligible [8].

2.2. LNSM

The strength of the transmitted signal is affected by many factors, such as reflection, scattering, and diffraction. At present, these three aspects of the impact on wireless channel propagation are mainly considered. Most wireless channel models combine theoretical and empirical values. The theoretical method depends on the measurement data, and the empirical method depends on the curve fitting.

In fact, through the measurement of the field environment, the channel model can be established and all the transmission factors in the channel can be taken into consideration, which is beneficial to improve the RSSI ranging accuracy. However, previous research data was based solely on the room / exterior environment of ZigBee wireless technology and did not fully adapt to the site bike environment. The circuit has a specific area shape

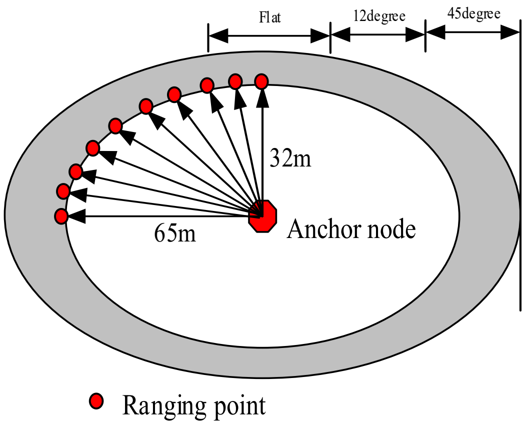

Fig. 1. Bike mode

The race track is a flat area, as shown in Figure 1. From the starting line to 25 meters is flat, then, the tilt angle increased from 12 degrees to 45 degrees slowly. The larger the tilt angle, the more the reflected signal, the worse the channel conditions. Most wireless ZigBee modules support RSSI, which means that you can measure the signal power of each packet. The transmitted signal power or energy is the signal parameter, which implies the distance information between nodes. The LNSM model is used to establish the relationship between distance and signal power [9], as shown in equation (3)

$$PL(d) = PL_0(d_0) + 10n\log_{10}(d/d_0) + X_\sigma \, . \tag{3}$$

Among which $PL(d)$ represents the path loss after signal transmission distance d. $PL_0(d_0)$ indicates the energy consumed by the signal over the reference distance, usually $d_0 = 1m$. n is the path loss index, and X_σ is a Gaussian random variable with zero mean and σ is the standard deviation.

Assuming that the signal power transmitted by the anchor node is P_t , then the RSSI value received by the mobile node [10]:

$$RSSI = P_t - PL(d) \, . \tag{4}$$

Substituting equation (3) into equation (4), the power of the signal received by the mobile node is finally obtained:

$$RSSI = P_t - PL_0(d_0) - 10n\log_{10}(d/d_0) + X_\sigma \, . \tag{5}$$

3. TCTR algorithm

3.1. Data transfer model

The data transfer model is shown in Figure 2, with one anchor node (coach) and four mobile nodes. Mobile nodes are installed in the car, and were a router node, three sensor nodes. Three sensor nodes measure speed, torque and rhythm respectively. All sensor nodes are wirelessly connected through the ZigBee network. The three sensor nodes use the router node to communicate with the anchor node and transmit data to it. The reason for using router nodes is that the three sensor nodes can not directly transmit the bicycle data to the anchor node.

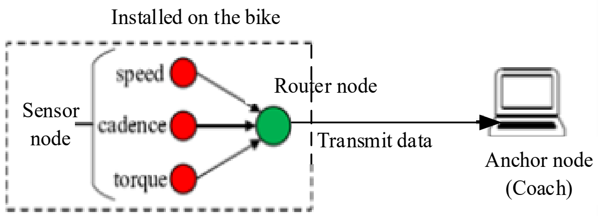

Fig. 2. Data transfer model

The anchor and router nodes are composed of a ZigBee transmitter and an Arduino Atmega 328p microcontroller. The anchor node is mounted on the ground surface at a height of about 1.5 meters from the ground. The router node is fixed on the bicycle seat with a height of about 0.85 Meter. Since the router node moves with the bike, hereinafter referred to as the mobile node and powered by the battery, the anchor node is powered by the USB cable.

3.2. Parameter Estimation

Use MATLAB7.1 software to establish a simulation platform, which will also establish two outdoor and indoor two experiments. Outdoor experiments are done at the outdoor venues for cycling, while the latter is done at the gymnasium. By measuring these two site data on the ground, their environmental parameters are estimated, ie indoor / outdoor PL_0, n and noise standard deviations σ, as shown in Eq. (5).

(1) indoor experimental environment

The indoor experiment was completed at the gymnasium. The gymnasium floor plan is shown in Figure 3, with an area of $36m \times 34m$, 6 anchor nodes (AN) were installed, with a diagonal distance of 32 meters. This experiment uses AN1 to measure the RSSI values at 13 locations on the diagonal.

(2) outdoor experimental environment

Outdoor experiments were done at the outdoor venues for cycling, with anchor nodes at the center of the site area, as shown in Figure 1. The mobile node moves along the bicycle track and receives the beacons packet from the anchor node to collect the RSSI data. The mobile node then uses the RSSI value to estimate the distance. The size of the bike yard area is $130m \times 65m$, and the length of the orbit is 333 meters.

As shown in Figure 1, the mobile node has the smallest distance from the anchor node through the field measurement, with the maximum distance being 32 meters and 65 meters respectively. During the experiment, the RSSI values were measured respectively at a predetermined 18 locations, as indicated by the dotted line head in FIG. 1.

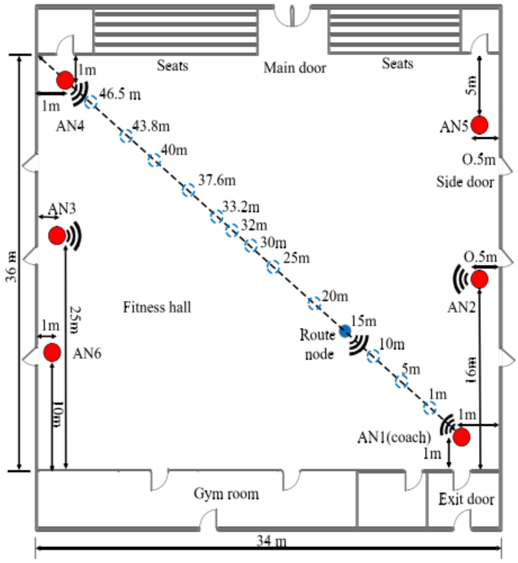

Fig. 3. Indoor experimental field

3.3. Experimental values

The XBees [11] for mobile nodes and anchor nodes were configured by using X-CTU software and the RSSI values were measured. The RSSI values were measured at 18 pre-determined outdoor locations and 13 indoor locations respectively, recording 20 times for each location. Sample one packet per second, each packet size is 34 bytes.

Figure 4 shows the experimental and theoretical RSSI values for outdoor and indoor experiments, where the theoretical value is obtained from Eq. (5). Figure 5 shows the success rate of mobile node receive data packet .

As can be seen from Figure 4, in the indoor environment, the measured RSSI value and the theoretical RSSI value can be consistent. In the outdoor environment, there is a large deviation between the measured RSSI value and the theoretical RSSI value, which is mainly due to the obstruction of signal transmission caused by objects such as indoor walls and windows.

In addition, mobile nodes in outdoor environments receive packets at higher rates than indoor environments. In addition, when the distance is less than 30 meters, the receiving rate of mobile nodes in the outdoor environment reaches 100% while that of the indoor environment fluctuates between 87 and 98%. This is mainly due to the reflection of transmitted signals by indoor objects.

3.4. Parameter Estimation Based on Fitting

Based on the measured experimental data, the environmental parameters were estimated. Fitted line was drawn by measuring the relationship between average

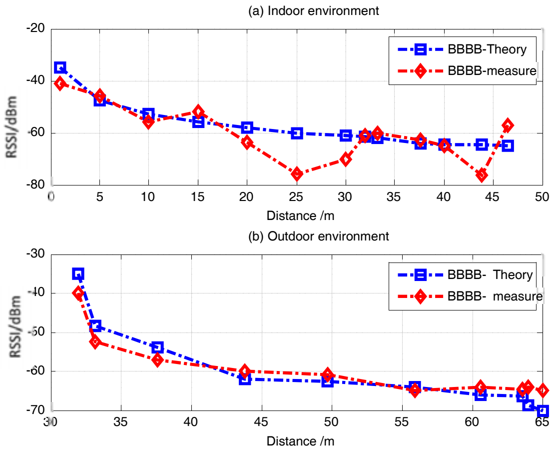

Fig. 4. RSSI value changes with the distance

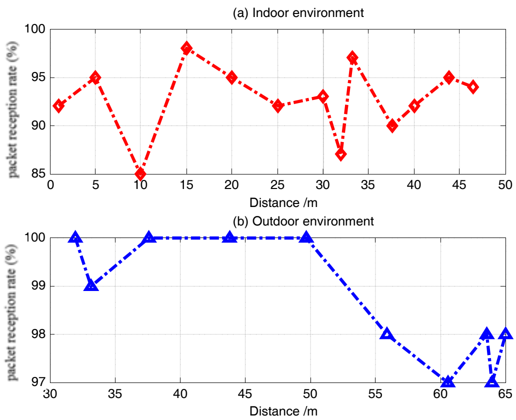

Fig. 5. packet reception success rate

RSSI value and distance. The regression line can be estimated by equations (6) and (7).

$$y_1 = -16.138x_1 - 39.801\,. \tag{6}$$

$$y_2 = -17.019x_2 - 38.883\,. \tag{7}$$

Where equation (6) is the outdoor environment, and equation (7) is the indoor environment. The y is the mean of RSSI, x is the logarithmic scale corresponding to the distance d. Therefore, equations (6) and (7) can be transformed into:

$$RSSI = -16.138\log\left(d/d_0\right) - 39.801\,. \tag{8}$$

$$RSSI = -17.019\log\left(d/d_0\right) - 38.883\,. \tag{9}$$

By comparing equations (8) and (9) with equation (5), the outdoor and indoor path fading indices and standard deviations can be estimated , as shown in Eqs. (10) and (11)

$$\begin{cases} 10n = 16.138 \\ P_t - PL_0 + X_\sigma = -39.801 \end{cases} \tag{10}$$

$$\begin{cases} 10n = 17.019 \\ P_t - PL_0 + X_\sigma = -38.883 \end{cases} \tag{11}$$

Finally, the parameters of the LNSM could be estimated, indoor / outdoor PL_0, n and noise standard deviations σ can be estimated as shown in Table 2, where the theoretical values are based on available literature. As can be seen from Table 2, there is a discrepancy between the estimated value of the field environment and the theoretical value, which also shows that it is inaccurate to use the theoretical environment parameter value as the environment parameter of the site bicycle.

Table 2. Environmental parameter estimates

Scenes		PL_0/dBm	n	σ / dB
Indoor scene	Theoretical value	37	1.8	2.0
	Estimated value	41.04	1.701	2.157
Indoor scene	Theoretical value	37	2.0	2.0
	Estimated value	39.35	1.613	0.451

3.5. Ranging mean square error

This section, through the field measurement of environmental parameters, ranging, and analysis of the accuracy of ranging. Root mean square error (RMSE) [12-16] is used to estimate the ranging accuracy of the algorithm, which is defined as shown in Eq. (12)

$$RMSE = \sqrt{\frac{1}{n}\sum_{i=1}^{n}(d_A - d_E)^2}. \tag{12}$$

In order to better analyze the accuracy of TCTR ranging, choose distance measurement based on theoretical parameter as a reference, and make a comparison. The experimental data of two algorithms are shown in Figure 6 and Figure 7. Select the theoretical environment parameters ranging algorithm as a reference, in the simulation diagram labeled TCTR-theoretical algorithm. The proposed TCTR algorithm uses the parameters estimated in Table 1. It mainly tests the ability to track the bike, that is, ranging accuracy in the indoor and outdoor environments.

Figure 6 plots the distance-dependent variation of the mean square ranging error between the TCTR-theoretical algorithm and the proposed TCTR algorithm for indoor and outdoor environments. As can be seen from Figure 7, compared with the TCTR-theory algorithm, the root mean square distance error of the proposed TCTR algorithm is effectively reduced. For example, when the ranging distance is equal to 30 meters, the root-mean-square error of TCTR is about 2.0 meters, while the root mean square distance error of TCTR-theory algorithm is about 5.02 meters.

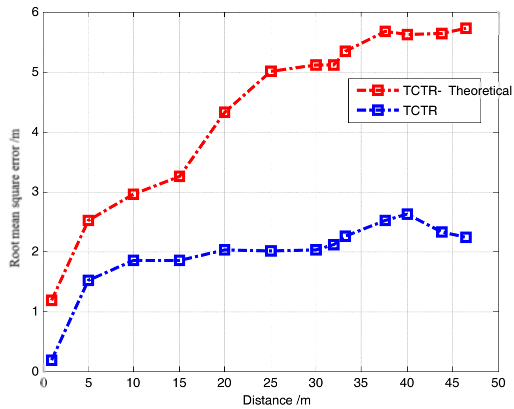

Fig. 6. Ranging root mean square error of indoor scene root mean square error

Figure 7 plots the distance-dependent variation of the root-mean-square distance measurement error of the TCTR-theoretical algorithm and the proposed TCTR algorithm in an outdoor scene environment. Similar to the simulation results in Figure 6, the mean square error of the TCTR algorithm is lower than that of the TCTR-theory algorithm. These data show that the accuracy of the proposed TCTR algorithm is higher than that of the TCTR-theory algorithm in both indoor and outdoor environments.

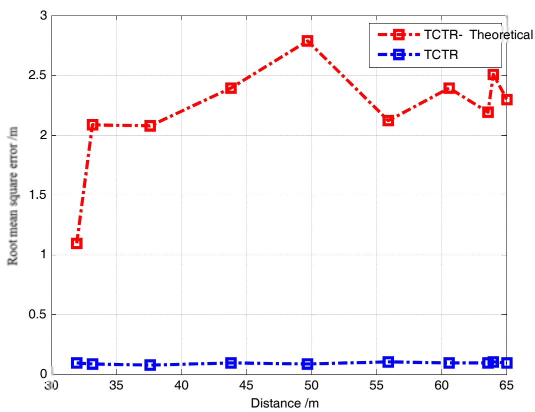

Fig. 7. Ranging root mean square error in outdoor scenes

4. Summary

In order to locate the race driver in real time to ensure their safety, a tracking algorithm based on Received Signal Strength Index (RSSI) ranging is proposed. The purpose of the TCTR algorithm is to estimate the distance between a mobile node (bicycle) and an anchor node (coach). First of all, the factors influencing the distance error based on RSSI are analyzed. Then the environment parameters are measured in real time, and then the environmental parameters are re-estimated. The estimated parameters are used to measure the distance. The indoor and outdoor environment experiments show that the proposed TCTR distance measurement algorithm can effectively estimate the environmental parameters and improve the accuracy of ranging, which can effectively track the bicycle.

Acknowledgement

Research on distributed social network structure, resource sharing and migration algorithm F020803.

References

[1] Y. J. Zhao, L. Wang, H. J. Wang, and C. J. Liu: *Minimum Rate Sampling and Spectrum Blind Reconstruction in Random Equivalent Sampling.* Circuits Systems and Signal Processing, *34* (2015), No. 8, 2667–2680.

[2] S. L. Fernandes, V. P. Gurupur, N. R. Sunder, N. Arunkumar, S. Kadry: *A novel nonintrusive decision support approach for heart rate measurement*, (2017) Pattern Recognition Letters. https://doi.org/10.1016/j.patrec.2017.07.002

[3] N. Arunkumar, K. Ramkumar, V. Venkatraman, E. Abdulhay, S. L. Fernandes, S. Kadry, S. Segal: *Classification of focal and non focal EEG using entropies.* Pattern Recognition Letters, *94* (2017), 112–117

[4] W. S. Pan, S. Z. Chen, Z. Y. Feng.: *Investigating the Collaborative Intention and Semantic Structure among Co-occurring Tags using Graph Theory.* International Enterprise Distributed Object Computing Conference, IEEE, Beijing, (2012), 190–195.

[5] Y. Z. Chen, F. J. Tang, Y. Bao, Ya. Tang, G. D. Chen: *A Fe-C coated long period fiber grating sensor for corrosion induced mass loss measurement.* Optics letters, *41* (2016), 2306–2309.

[6] N. Arunkumar, S. Jayalalitha, S. Dinesh, A. Venugopal, D. Sekar: *Sample entropy based ayurvedic pulse diagnosis for diabetics*, IEEE-International Conference on Advances in Engineering, Science and Management, ICAESM-2012, (2012), art. No. 6215973, 61–62.

[7] J. W. Chan, Y. Y. Zhang, and K. E. Uhrich: *Amphiphilic Macromolecule Self-Assembled Monolayers Suppress Smooth Muscle Cell Proliferation*, Bioconjugate Chemistry, *26* (2015), No. 7, 1359–1369.

[8] M. P. Malarkodi, N. Arunkumar, V. Venkataraman: *Gabor wavelet based approach for face recognition*, International Journal of Applied Engineering Research, *8* (2013), No. 15, 1831–1840.

[9] L. R. Stephygraph, N. Arunkumar: *Brain-actuated wireless mobile robot control through an adaptive human-machine interface*, Advances in Intelligent Systems and Computing, *397* (2016), 537–549.

[10] N. Arunkumar, V. Venkataraman, T. Lavanya: *A moving window approximate entropy based neural network for detecting the onset of epileptic seizures*, International Journal of Applied Engineering Research, *8* (2013), No. 15, 1841–1847.

[11] J. W. Chan, Y. Y. Zhang, and K. E. Uhrich: *Amphiphilic Macromolecule Self-Assembled Monolayers Suppress Smooth Muscle Cell Proliferation*, Bioconjugate Chemistry, *26* (2015), No. 7, 1359–1369.

[12] Y. Y. Zhang, Q. Li, W. J. Welsh, P. V. Moghe, and K. E. Uhrich: *Micellar and Structural Stability of Nanoscale Amphiphilic Polymers: Implications for Anti-atherosclerotic Bioactivity*, Biomaterials, *84* (2016), 230–240.

Received May 7, 2017